J Therm Anal Calorim (2015) 122:571–578
DOI 10.1007/s10973-015-4811-x

Thermolysis mechanism of dysprosium hexahydrate nitrate $Dy(NO_3)_3{\cdot}6H_2O$ and modeling of intermediate decomposition products

P. Melnikov[1] · I. V. Arkhangelsky[2] · V. A. Nascimento[1] · A. F. Silva[1] · L. C. S. de Oliveira[3] · L. Z. Zanoni Consolo[1] · A. S. Herrero[3]

Received: 23 March 2015 / Accepted: 27 May 2015 / Published online: 24 June 2015

Abstract The thermal decomposition of dysprosium nitrate is a complex process which begins with the simultaneous condensation of the initial monomer $Dy(NO_3)_3{\cdot}6H_2O$ into a cyclic hexamer $6[Dy(NO_3)_3{\cdot}6H_2O]$. This cluster gradually loses water and nitric acid, and intermediate oxynitrates $Dy_6O_7(NO_3)_4{\cdot}6H_2O$ and $Dy_6O_8(NO_3)_2{\cdot}5H_2O$ are formed. At higher temperatures, these products undergo further degradation, lose nitrogen dioxide, water, and oxygen, and finally, after having lost lattice water, are transformed into the cubic form of dysprosium oxide. The models of intermediate oxynitrates represent a reasonably good approximation to the real structures and a proper interpretation of experimental data. The comparison of the potential energies of consecutive oxynitrates permitted an evaluation of their stability. The mechanism was studied by thermal analysis, differential scanning calorimetry, infrared spectroscopy, and X-ray diffraction. The mass losses were related to the vibrational energy levels of the evolved gases.

Keywords Rare earth · Dysprosium nitrate hexahydrate · Thermal decomposition · Oxynitrates · Computer modeling

✉ P. Melnikov
petrmelnikov@yahoo.com

[1] School of Medicine, UFMS, Caixa Postal 549, Campo Grande, MS, Brazil

[2] School of Chemistry, Moscow State University, Vorobievy Gory, 119517 Moscow, Russia

[3] School of Chemistry, Federal University of Mato Grosso do Sul, Caixa Postal 549, Campo Grande, MS, Brazil

Introduction

A study of rare earth nitrates $Ln(NO_3)_3{\cdot}6H_2O$ thermal stability has been recently carried out for a number of elements of the lanthanide series [1–3], as well as other elements with charge 3^+, including gallium [4], aluminum [5], chromium (III) [6], and iron (III) [7, 8]. A common feature for their thermolysis is a complex condensation process generating a tetramer arrangement formed by alternating metal and oxygen atoms. Soon after that, the resulting tetramer heterocycle gradually loses water, nitric acid, and nitrogen oxides, and through the formation of unstable oxynitrates is converted into Me_2O_3. It was also shown that this mechanism does not involve the formation of simple oxynitrates $Me^{III}ONO_3$ or anhydrous salts as has been suggested elsewhere [9, 10]. Recently, an investigation has been published on thermal stability of samarium nitrate showing that this is markedly different from the processes described above because of the lower basicity of the element and distinct mechanism of inner hydrolysis. Actually, the existence of intermediate structures with six atoms of samarium best fitted the experimental results that the tetrahedral model [11].

Dysprosium nitrate hexahydrate $Dy(NO_3)_3{\cdot}6H_2O$ crystallizes in a triclinic system, space group PI. In this structure, each of the Dy(III) ions is coordinated by ten oxygen atoms of three nitrate groups and six water molecules forming a distorted icosahedron (Fig. 1).

As both dysprosium and samarium pertain to the lanthanide row and have close ionic radii, there are all grounds to suggest that thermal behavior of dysprosium nitrate must resemble that of $Sm(NO_3)_3{\cdot}6H_2O$. In the same work [11], the molecular mechanics technique was used for comparing the potential energies of consecutive products of thermal decomposition to build up feasible models of unstable

Fig. 1 Inner coordination shell of $Dy(NO_3)_3{\cdot}6H_2O$ [12]

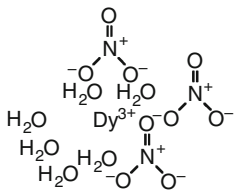

compounds that form during the thermolysis. Force field methods [13] used to predict the structures gave a very satisfactory description of the geometry of the intermediate compounds.

The aim of the present work is to apply hypothesis of hexamer structures for the interpretation of the thermogravimetry curves of $Dy(NO_3)_3{\cdot}6H_2O$ and select appropriate models for the products of its thermal decomposition. It intends to deal with the scarcity of experimental structural information on samarium oxynitrates, as an option to fill the gap.

Materials and methods

The starting reagent used was dysprosium nitrate hexahydrate $Dy(NO_3)_3{\cdot}6H_2O$, of analytical grade purity (99.9 %), purchased from Sigma-Aldrich. Direct heating of the commercial reagent resulted in mass loss of 58.21 % confirming the water number slightly lower than six (calc. 59.31 %). Visual observations were carried out in air, using a platinum receptacle, from room temperature to 300 °C. Thermal gravimetric analysis (TG) and differential scanning calorimetry (DSC) were used to study thermal behavior, employing a 50H Shimadzu Instrumentation and Netsch STA Jupiter 449C Instrumentation. Test specimens, in the first case, were heated in a flux of nitrogen (temperature range from −40 to 500 °C), and in the second case in a flux of argon (temperature range from 25 to 500 °C), always at a heating rate of 5 °C min^{-1}. Mass losses during heating were analyzed and compared to previously calculated values. Melting point, gas liberation, and crystallization processes were additionally monitored by visual observation, allowing the visualization of NO_2 vapors and other peculiarities. The evolution of volatiles was measured using a Netsch STA Jupiter 449C apparatus coupled with a FTIR spectrometer. Infrared spectroscopy of evolved gases was performed using a Tensor 27 Bruker spectrometer. The spectra were detected in a range 400–4000 cm^{-1}. Temperature of the transport gas line was 240 °C. The spectra were taken for 12 s at a frequency accuracy of 1 cm^{-1}. The identification of the IR spectra was done on the basis of NIST Chemistry WebBook [14]. The samples were previously sealed in glass ampoules in a hot condition in order to avoid the impact of water vapors from the air. X-ray powder pattern of solid sample was registered with a Siemens Kristalloflex diffractometer (CuKα radiation) with a graphite diffracted beam monochromator and Ni filter. Data were collected in the range of $2\theta = 4°–70°$ with a scan step $2\theta = 0.02°$ and scan rate of 18 min^{-1}. Phase identification was performed using ICDD PDF-2 database. In this work, compounds were simulated using the standard HYPERCHEM 7.5 software package employing MM+ force field program [13].

Results and discussion

Thermal analysis

As established by visual observations, the compound turns into a clear liquid at around 55 °C similar to other nitrate hexahydrates. This liquid begins to boil at ~122 °C, and immediately, the smell of gaseous HNO_3 starts to feel. The solidification/crystallization becomes noticeable at ~220 °C, and then at ~350 °C, nitrogen dioxide fumes are released.

The DSC analysis of $Dy(NO_3)_3{\cdot}6H_2O$ is presented in Fig. 2. From approximately 36 °C on, a series of endothermic effects become evident, reflecting the dehydration/decomposition processes. Along with TG pattern, their analysis can be used for a rigorous interpretation of results.

The representative TG curve of $Dy(NO_3)_3{\cdot}6H_2O$ is shown in Fig. 3 in comparison with the analogous curve of $Sm(NO_3)_3{\cdot}6H_2O$ from our recent publication [11]. It can be seen that despite the obvious similarities, they differ markedly in the early stages of thermal decomposition, splitting of the major peak at ~366 °C and other peculiarities. Hence, the interpretation of samarium effects cannot be transferred straightforwardly to dysprosium compound.

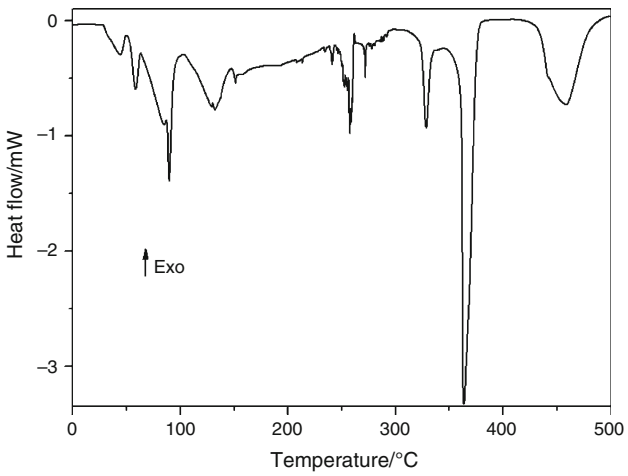

Fig. 2 DSC curve of $Dy(NO_3)_3{\cdot}6H_2O$

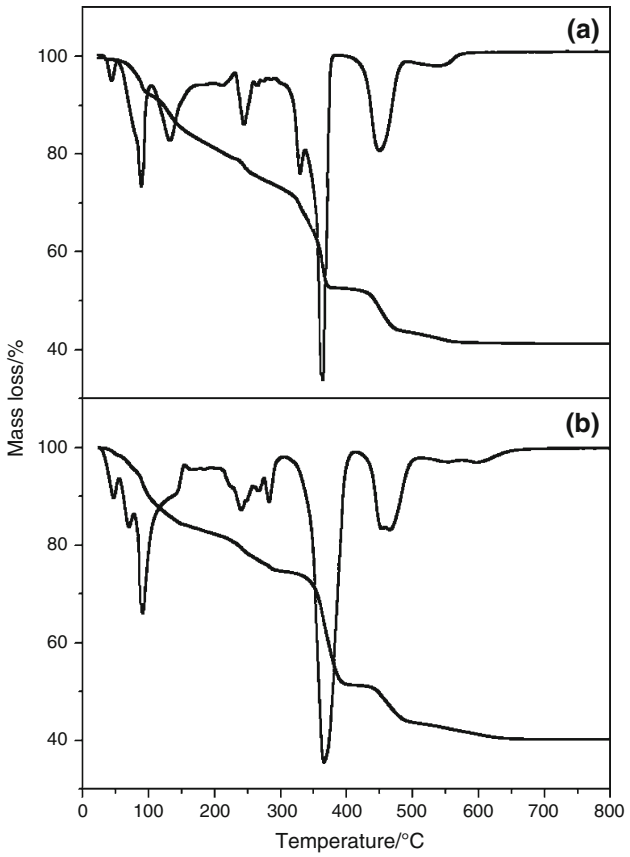

Fig. 3 TG and DTG curves of $Dy(NO_3)_3 \cdot 6H_2O$ (**a**) compared with $Sm(NO_3)_3 \cdot 6H_2O$ (**b**)

It is well known that the decomposition onset for the nitrates of trivalent metals is generally below 100 °C. In this respect, dysprosium nitrate is not an exception: The first mass loss is due to water evaporation after fusion of the original hexahydrate at 48–52 °C. Between 48 and 127 °C, the compound loses 15.1 % of mass, corresponding to 23 mol of water, taking into account the presence of six monomers at the start of decomposition process. Then, between 127 and 322 °C occurs mass loss corresponding to 14 mol of nitric acid.

As in the case of samarium, our working hypothesis was that dysprosium nitrate would be hydrolyzed by the crystallization water, and as a result, nitric acid should have been produced. Indeed, this acid, or rather the azeotrope 68 % HNO_3–32 % H_2O, is detected by the IR sensor of the volatile products during the thermal treatment. Nitric acid is identified by its characteristic absorption bands at 892, 1319, 1508, 1596, 1631, and 1716 cm^{-1} (Fig. 4). It is clearly seen that the two releases of nitric acid are accompanied by net endothermic effects on DSC curve, with onsets at 242 and 316 °C, respectively. The 3D diagram of IR spectrum shown in Fig. 5 gives a general view of absorption at sequential temperatures.

So, at least up to 220 °C we do not have the ability to judge about precise compositions, since the mixture is in the liquid state, and the removal of HNO_3 is essentially a continuous process, so solid phases cannot be isolated and identified. It would be reasonable to assume that the pyrolysis curve reflects the presence of various chemical products, not single stoichiometric compounds of definite composition. Table 1 shows the compositions of the reaction products with expected and experimentally found mass losses at different stages of thermal treatment.

Between 320 and 474 °C, the solid product loses 9.2 % of mass, possibly in two substeps. At this step, the composition of the gaseous phase changes. The observation of the characteristic brown color of nitrogen dioxide and the known instability of HNO_3 at high temperatures suggest that the acid is not actually present in its molecular form. Actually, thermal decomposition of nitric acid is a reversible endothermic reaction and almost quantitatively proceeds according to the equation [15]:

$$HNO_3 = NO_2 + 0.5H_2O + 0.25O_2 + 7.8 \text{ kcal mol}^{-1} \quad (1)$$

As can be seen from dynamics of nitrogen dioxide removal (Fig. 6) in relation to DSC curve, and from the 3D diagram of IR spectrum (Fig. 5), at 425 the sensor detects characteristic absorbance bands of nitrogen dioxide 1597, 1629, and 1716 cm^{-1}. Another product of HNO_3 thermal disproportionation is oxygen, but this element in principle cannot be registered in the spectrum due to the lack of changing dipole moment. The next loss of mass (2.63 %) takes place around 650 °C, corresponding to the removal of remaining $4H_2O$, and the process is completed. The diffractogram given in Fig. 7 matches the pattern of the cubic dysprosium oxide, Dy_2O_3 (ICSD file 082241).

To the best of our knowledge, the X-ray structure determination for dysprosium oxynitrates has never been performed. So the thermal analysis suggests the following sequence of structural transformations. The removal of HNO_3 and the corresponding amount of water lead to creation of oxygen bridges between the dysprosium atoms, obliging $6Dy(NO_3)_3$ to condense into a hexamer structure $Dy_6O_6(NO_3)_6 \cdot 13H_2O$ (Scheme Fig. 8a). Calculations show that the hypothesis concerning cluster preexistence in the solid state is quite applicable to the present case of dysprosium nitrate hydrate. This is corroborated by the structures of hexanuclear complexes containing six dysprosium atoms proposed as single molecule magnets [16–18]. Simultaneously, the entire system of hydrogen bonds is rebuilt.

Both DTG and DSC curves show that this is a complex step-wise process, and the water belongs to differently bonded species which are involved in intermolecular hydrogen bonding, making the monomers stand together. At the following stage, the hexamer loses 1 mol of water,

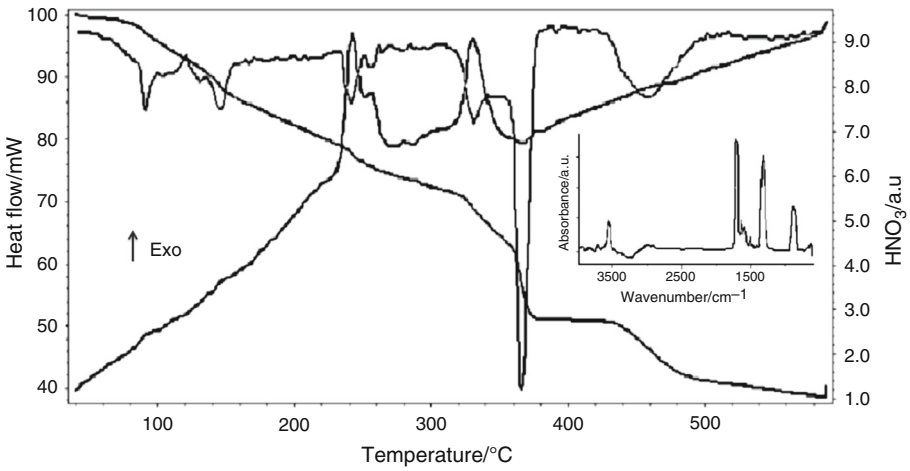

Fig. 4 Dynamics of nitric acid removal in relation to TG and DSC curves. HNO_3 spectrum is used as reference (*inset*)

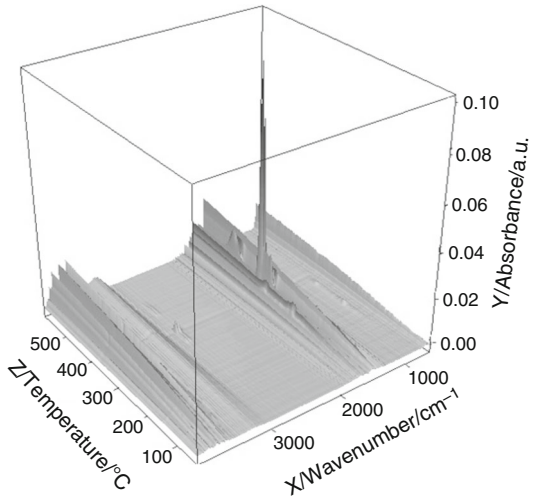

Fig. 5 Temperature-dependent 3D diagram of IR spectra of the $Dy(NO_3)_3{\cdot}6H_2O$ thermal decomposition

2 mol of nitrogen dioxide, and 1 mol of oxygen, so the composition of the resulting solid product corresponds to $Dy_6O_7(NO_3)_4{\cdot}6H_2O$ (Scheme Fig. 8b) with the single cross-linking bridge Dy–O–Dy. This hexamer, in turn, loses the same amount of volatile products, giving $Dy_6O_8(NO_3)_2{\cdot}5H_2O$ with two internal bridges (Scheme Fig. 8c). Denitrification then ends with the formation of an unstable hydrate $Dy_6O_9{\cdot}4H_2O$ (Scheme Fig. 8d), which loses remaining water, and there are no further thermal transformations. These features are reminiscent of the process of samarium nitrate thermolysis, where the intermediate oxynitrates were shown to be identical in composition [11]. So, the whole process can be described as:

$$6\left[Dy(NO_3)_3{\cdot}6H_2O\right] = 3Dy_2O_3 + 14HNO_3 + 4NO_2 + O_2 + 29H_2O \quad (2)$$

Structural modeling

The models obtained using the molecular mechanics technique are shown in Figs. 9–12. The calculated interatomic distances are presented in Table 2. We did not perform any systematic energy sampling for searching conformational energy space. As can be seen from Fig. 9, the base of the hexamer is formed by an inorganic heterocycle composed of six atoms of dysprosium, alternating

Table 1 Mass losses at different stages of $Dy(NO_3)_3{\cdot}6H_2O$ pyrolysis and composition of the volatile products in relation to the initial six monomers

Steps	Compositions	Loss of volatile products/mol				Mass loss/%	
		Water	Nitric acid	Nitrogen dioxide	Oxygen	Exp.	Calc.
1	$3Dy_2O_3{\cdot}9N_2O_5{\cdot}36H_2O$	23	–	–	–	15.1	15.38
2	$3Dy_2O_3{\cdot}9N_2O_5{\cdot}13H_2O$	–	14	–	–	32.20	32.20
3	$3Dy_2O_3{\cdot}2N_2O_5{\cdot}6H_2O$	1	–	2	1	9.20	8.96
	$3Dy_2O_3{\cdot}N_2O_5{\cdot}5H_2O$	1	–	2	1		
4	$3Dy_2O_3{\cdot}4H_2O$	4	–	–	–	2.63	2.6
	$3Dy_2O_3$						

Total: $29H_2O$, $14HNO_3$, $4NO_2$, 2O

Final product: $3Dy_2O_3$

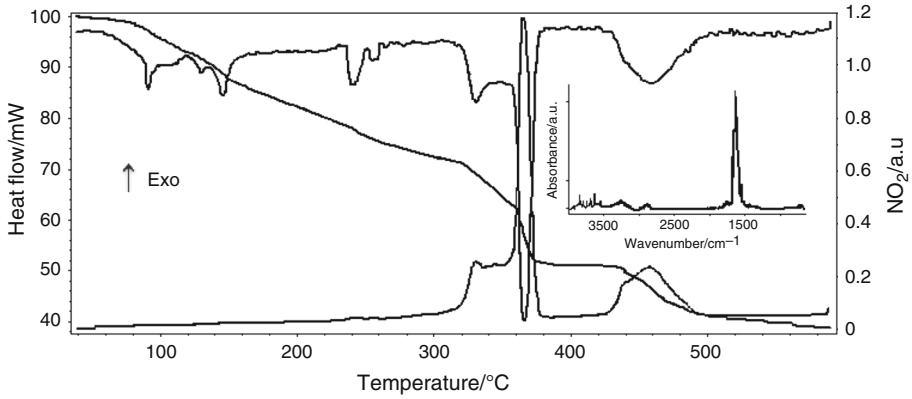

Fig. 6 Dynamics of nitrogen dioxide removal in relation to TG and DSC curves. The NO_2 spectrum is used as reference (*inset*)

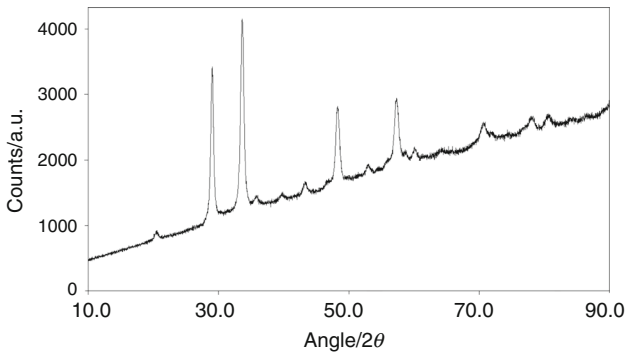

Fig. 7 Diffractogram of the sample heated at 650 °C

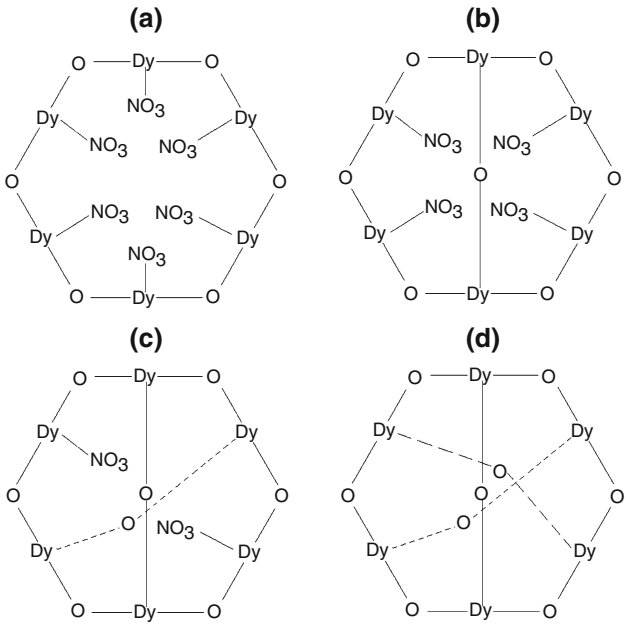

Fig. 8 Scheme showing the condensation process of $Dy_6O_6(NO_3)_6{\cdot}13H_2O$. Initial hexamer (**a**); intermediate oxynitrates (**b**, **c**); final hypothetical intermediate hexamer Dy_6O_9 (**d**). Hydrate water is omitted

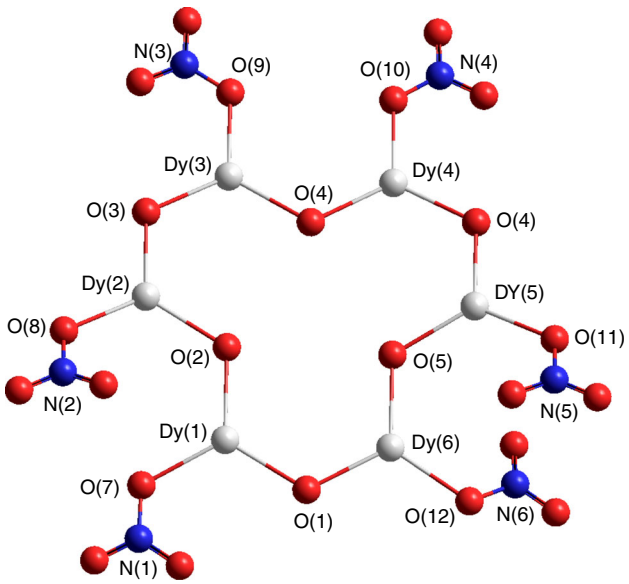

Fig. 9 Hexamer model of symmetric rotamer $Dy_6N_6O_{24}$

with six atoms of oxygen which, to simplify things, are numbered from 1 to 6. Together they form a rather symmetric crown-like cycle, wherein six dysprosiums and six oxygens sit in slightly different parallel planes, one anterior and the other posterior. The potential energy calculated for this structure is -0.131 kJ mol^{-1}.

Since the bonds Dy–O forming the cycles are not covalent, but rather ionic in nature, it becomes quite clear that, in contrast to the planar benzene ring, these cycles can easily become corrugated. Moreover, as the angle of this 'folding' may vary within certain limits, one can expect to find the presence of conformational isomers with slightly differing values of potential energy. In a real solid, this degree of freedom is unlikely to be preserved due to the requirements imposed by the densest packing. The same is true of the degree of freedom of rotation about the bonds between dysprosium and oxygen of NO_3^- groups attached

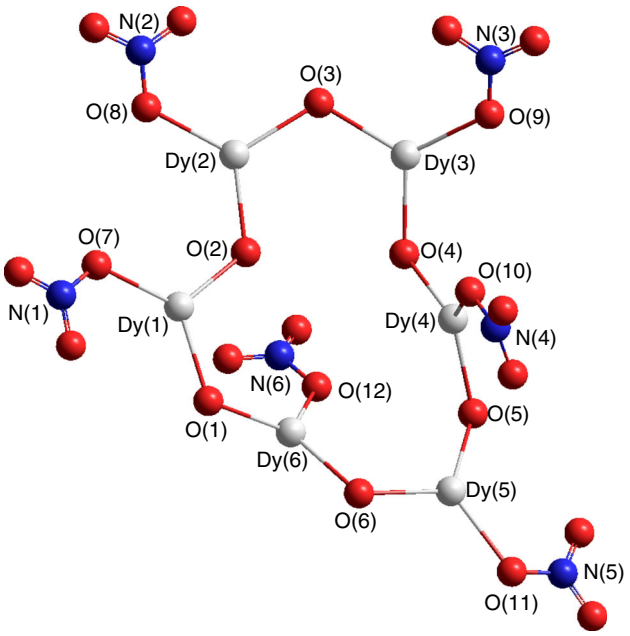

Fig. 10 Hexamer model of asymmetric rotamer $Dy_6N_6O_{24}$

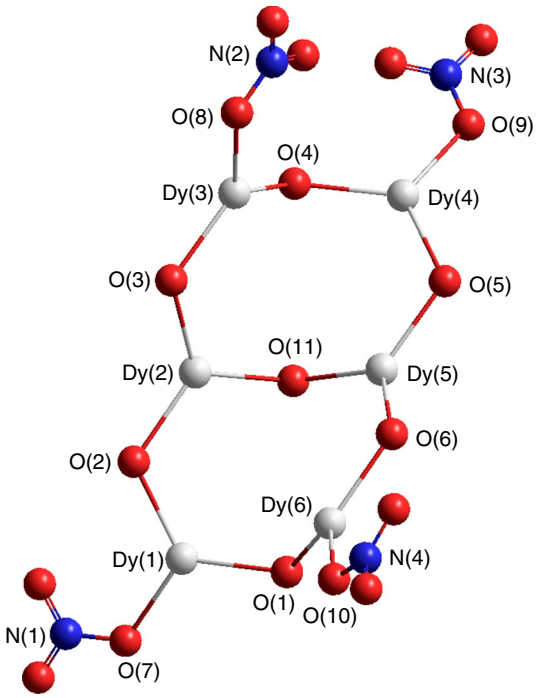

Fig. 11 Hexamer model of the rotamer $Dy_6N_4O_{19}$ with the bridge Dy(2)–O(11)–Dy(5)

to dysprosium atoms. These groups behave as slightly deformed nitrate anions with two external N=O bonds in the range of 1.29–1.30 Å and a short bond of 1.17 Å connecting to dysprosium. Meanwhile, the bond angles O–N–O found for the model are equal to the angles in solid nitrates (close to 120.0°) in accordance with the actual

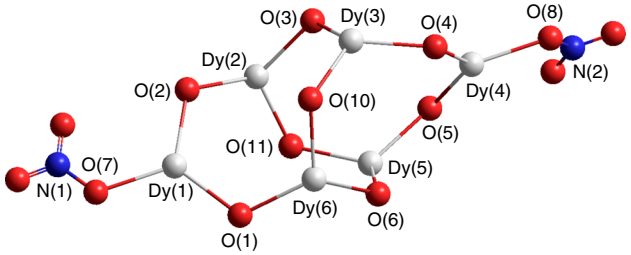

Fig. 12 Hexamer model of the rotamer $Dy_6N_2O_{14}$ with the two bridges, Dy(2)–O(11)–Dy(5) and Dy(3)–O(10)–Dy(6)

structure of the polyatomic ion which has trigonal planar geometry [19].

It is noteworthy that the rotation is accompanied by deformation of the cycle, as evidenced by the change in Dy–Dy distances from one isomer to the other. One of the deformed conformers is shown in Fig. 10. As can be seen from Table 2, the distances Dy–O are identical in both rotamers, that is, 2.27 Å. The comparison shows that they are much shorter than those refined from X-ray diffraction data for dysprosium oxide, that is, 2.56 Å [20].

Figure 11 shows the structure $Dy_6N_4O_{19}$ that might be formed after the removal of 2 mol of NO_2 and 1 mol of oxygen, so only four NO_3 groups would be bonded to the cycle. In this instance, a newly formed cross-bridge connects dysprosium atoms 2 and 5. As can be concluded from Table 2 and Fig. 11, some distances Dy–Dy are getting shorter and others larger, thus reflecting the increasing deformation of the cycle. The potential energy calculated for this structure is -26.30 kJ mol^{-1}. So, further condensation with removal of the distant NO_3 groups becomes more difficult to achieve, hence the slow kinetics. Anyway, the formation of the second bridge between Dy(3) and Dy(6) takes place, and the structure loses any resemblance to the original arrangement (Fig. 12). The potential energy calculated for this structure is -69.59 kJ mol^{-1}.

In view of the exceptional narrowness of the internal space, the formation of a third bridge (Fig. 13) does not seem probable. That is why the elimination of the last $2NO_3$ instead of metastable Dy_6O_{18} will produce 3 mol of Dy_2O_3, in agreement with the experimental data. The potential energy calculated for Dy_6O_{18} hypothetical structure is 206.64 kJ mol^{-1}.

The calculation of minimal potential energies for the aforementioned models shows that, in an arbitrary scale, their numerical values increase considerably with the number of oxygen bridges. This is a clear indication that the stability of the related structures decreases from the original hexamer to the product devoid of nitrogen. The exceptionally high level of potential energy for a hypothetical Dy_6O_9 (206.64 kJ mol^{-1}) shows that the existence of such a compound is really questionable. It is clear that the levels of potential energy, calculated by means of

Table 2 Interatomic distances (Å) calculated for hexamer models

Distances	$Dy_6N_6O_{24}$ sym	$Dy_6N_6O_{24}$ asym	$Dy_6N_2O_{14}$	Dy_6O_{18}
Dy(1)–O(1)	2.27	2.27	2.27	2.25
Dy(1)–O(2)	2.26	2.27	2.27	2.26
Dy(2)–O(2)	2.26	2.27	2.27	2.26
Dy(2)–O(3)	2.27	2.27	2.27	2.30
Dy(3)–O(3)	2.27	2.27	2.27	2.30
Dy(3)–O(4)	2.27	2.27	2.27	2.27
Dy(4)–O(4)	2.27	2.27	2.27	2.27
Dy(4)–O(5)	2.27	2.27	2.27	2.27
Dy(5)–O(5)	2.27	2.27	2.27	2.27
Dy(5)–O(6)	2.27	2.27	2.27	2.27
Dy(6)–O(6)	2.27	2.27	2.27	2.27
Dy(6)–O(1)	2.27	2.27	2.27	2.27
Dy(1)–O(7)	2.27	2.27	2.27	–
Dy(2)–O(8)	2.27	–	–	–
Dy(3)–O(9)	2.27	2.27	–	–
Dy(4)–O(10)	2.27	2.27	2.27	2.27
Dy(5)–O(11)	2.27	2.27	2.27	2.30
Dy(6)–O(12)	2.27	2.27	2.27	2.29
Dy(1)–Dy(2)	4.00	3.89	3.92	3.04
Dy(1)–Dy(3)	6.49	7.23	5.84	4.62
Dy(1)–Dy(4)	6.28	8.90	8.60	4.36
Dy(1)–Dy(5)	7.39	5.73	5.84	3.50
Dy(1)–Dy(6)	3.81	3.97	3.92	3.20
Dy(2)–Dy(3)	3.88	3.90	3.86	4.19
Dy(2)–Dy(4)	6.15	5.76	5.84	3.51
Dy(2)–Dy(5)	9.05	3.89	3.86	4.24
Dy(2)–Dy(6)	6.45	4.83	4.51	5.43
Dy(3)–Dy(4)	3.93	3.93	3.92	3.20
Dy(3)–Dy(5)	7.77	4.80	4.50	5.43
Dy(3)–Dy(6)	6.91	7.32	3.86	4.14
Dy(4)–Dy(5)	3.93	3.89	3.92	3.04
Dy(4)–Dy(6)	4.49	3.93	5.84	4.63
Dy(5)–Dy(6)	3.82	3.96	3.86	4.19
N(1)–N(2)	6.61	–	–	–
N(1)–N(3)	11.27	13.11	–	–
N(1)–N(4)	9.77	14.12	14.58	–
N(1)–N(5)	13.17	–	–	–
N(1)–N(6)	7.08	9.25	–	–
N(2)–N(3)	7.88	–	–	–
N(2)–N(4)	10.61	–	–	–
N(2)–N(5)	15.10	–	–	–
N(2)–N(6)	7.72	–	–	–
N(3)–N(4)	6.53	12.98	–	–
N(3)–N(5)	6.98	–	–	–
N(3)–N(6)	8.39	10.98	–	–
N(4)–N(5)	6.39	–	–	–
N(4)–N(6)	6.97	12.98	–	–
N(5)–N(6)	8.31	–	–	–

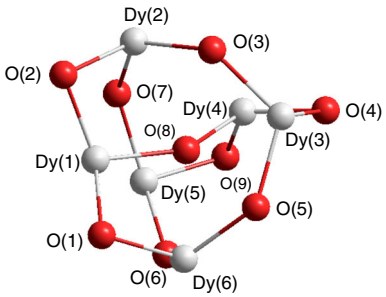

Fig. 13 Hypothetical hexamer model of Dy_6O_9, with the three bridges

molecular mechanics, must not necessarily have any definite physical meaning in themselves. However, when considering a series of related structures, the method may be of help when interpreting the experimental findings in the absence of X-ray data for the interatomic distances and bond angles.

Conclusions

1. The thermal decomposition of dysprosium nitrate is a complex process, which begins with the simultaneous condensation of the initial monomer $Dy(NO_3)_3{\cdot}6H_2O$ into a cyclic hexamer $6[Dy(NO_3)_3{\cdot}6H_2O]$.
2. This hexamer gradually loses water and nitric acid, and intermediate oxynitrates $Dy_6O_7(NO_3)_4{\cdot}6H_2O$ and $Dy_6O_8(NO_3)_2{\cdot}5H_2O$ are formed.
3. At higher temperatures, these products undergo further degradation, lose nitrogen dioxide, water, and oxygen, and finally, after having lost lattice water, are transformed into the cubic form of dysprosium oxide.
4. The models of intermediate oxynitrates represent a reasonably good approximation to the real structures and a proper interpretation of experimental data.
5. The comparison of the potential energies of consecutive oxynitrates permitted an evaluation of their stability.

Acknowledgements The authors are indebted to CNPq and FUNDECT (Brazilian agencies) for financial support.

References

1. Melnikov P, Nascimento VA, Zanoni Consolo LZ. Computerized modeling of intermediate compounds formed during thermal decomposition of gadolinium nitrate hydrate. Russ. J Phys Chem. 2012;86:1659–63.
2. Melnikov P, Nascimento VA, Consolo LZZ, Silva AF. Mechanism of thermal decomposition of yttrium nitrate hexahydrate $Y(NO_3)_3{\cdot}6H_2O$ and modeling of intermediate oxynitrates. J Therm Anal Calorim. 2013;111:115–9.
3. Melnikov P, Nascimento VA, Arkhangelsky IV, de Oliveira LCS, Silva AF, Zanoni Consolo LZ. Thermogravimetric study of the scandium nitrate hexahydrate thermolysis and computer modeling of intermediate oxynitrates. J Therm Anal Calorim. 2015;119:1073–9.
4. Melnikov P, Nascimento VA, Zanoni Consolo LZ. Thermal decomposition of gallium nitrate hydrate and modeling of thermolysis products. J Therm Anal Calorim. 2012;107:1117–21.
5. Melnikov P, Nascimento VA, Arkhangelsky IV, Zanoni Consolo LZ. Thermal decomposition mechanism of aluminum nitrate octahydrate and characterization of intermediate products by the technique of computerized modeling. J Therm Anal Calorim. 2013;111:543–8.
6. Melnikov P, Nascimento VA, Arkhangelsky IV, Zanoni Consolo LZ, de Oliveira LCS. Thermolysis mechanism of chromium nitrate nonahydrate and computerized modeling of intermediate products. J Therm Anal Calorim. 2013;114:1021–7.
7. Wieczorek-Ciurowa K, Kozak AJ. The thermal decomposition of $Fe(NO_3)_3{\cdot}9H_2O$. J Therm Anal Calorim. 1999;58:647–51.
8. Melnikov P, Nascimento VA, Arkhangelsky IV, Zanoni Consolo LZ, de Oliveira LCS. Thermal decomposition mechanism of iron(III) nitrate and characterization of intermediate products by the technique of computerized modeling. J Therm Anal Calorim. 2014;115:145–51.
9. Berberini V, Milanese C, Bruni G, Marini A. Thermal decomposition of gallium nitrate hydrate $Ga(NO_3)_3{\cdot}xH_2O$. J Therm Anal Calorim. 2003;82:401–7.
10. Wendlandt WW, Sewell RG. The fusion temperatures of the rare earth chlorides and nitrate hydrates. Tex J Sci. 1961;8:231–4.
11. Melnikov P, Arkhangelsky IV, Nascimento VA, Silva AF, Zanoni Consolo LZ. Thermolysis mechanism of samarium nitrate hexahydrate. J Therm Anal Calorim. 2014;118:1537–41.
12. Shengli G, Huairang M, Zupel Y. Crystal structure of dysprosium (III) nitrate hexahydrate. J Northwest Univ (Natural Science Edition). 1990;20:53–8.
13. HyperChem for Windows, Tools for Molecular Modeling, Release 7.5, Hypercube Inc; 1115 4th Street, Gainsville, Florida 32601, USA, 2003.
14. NIST chemistry WebBook, NIST standard reference database number 69. www.http//webbook.nist/chemistry. Accessed 28 Nov 2014.
15. Manelis GB, Nazin GM, Rubtsov YuT, Strunin VA. Thermal decomposition and combustion of explosives and propellants. Boca Raton: CRC Press; 2003.
16. Tian H, Wang M, Zhao L, Guo YN, Guo Y, Tang J, Liu Z. A discrete dysprosium trigonal prism showing single-molecule magnet behavior. Chem Eur J. 2012;18:442–5.
17. Costes JP, Duhayon C. An ionic dysprosium complex made of a hexanuclear Dy_6 cationic cluster and a mononuclear Dy anionic unit. Eur J Inorg Chem. 2014;2014:4745–9.
18. Tian H, Guo YN, Zhao L, Tang J, Liu Z. Hexanuclear dysprosium (III) compound incorporating vertex- and edge-sharing Dy_3 triangles exhibiting single-molecule-magnet behavior. Inorg Chem. 2011;50:8688–90.
19. Wells AF. Structural inorganic chemistry. 5th ed. London: Oxford University Press; 1984.
20. Bartos A, Lieb KP, Uhmacher M, Wiarda D. Refinement of atomic positions in bixbyite oxides using perturbed angular correlation spectroscopy. Acta Cryst B. 1993;49:165–9.